

Inhibitive Effect on the Rate of Hydrolysis of Tetracaine by the Surfactant-Coated Magnetic Nanoparticles (Fe_3O_4)

Mohd Shaban Ansari, Kashif Raees, M. Z. A. Rafiquee*

Department of Applied Chemistry, Z.H. College of Engineering and Technology, Aligarh Muslim University, Aligarh 202002, Uttar Pradesh, India

*Corresponding author: E-mail: drrafiquee@gmail.com

DOI: 10.5185/amlett.2021.041619

The influence of the magnetic nanoparticles Fe_3O_4 and surfactant coated nanoparticles on the rate of alkaline hydrolysis of tetracaine were investigated spectrophotometrically. The Fe_3O_4 nanoparticles were synthesized by co-precipitation method. These synthesized nanoparticles were characterized by physical techniques. The XRD patterns showed the crystalline nature and the presence of two bands at 635 cm^{-1} and 585 cm^{-1} were assigned to the Fe-O bond vibrations in Fe_3O_4 . The SEM and TEM studies confirmed the spherical structure of nanoparticles. The VSM studies show the magnetic nature. The reaction rate increased linearly with increase in $[\text{NaOH}]$. The rate constant values decreased with the increase in the SDS coated Fe_3O_4 nanoparticles from $4.0 \times 10^{-4}\text{ s}^{-1}$ to $1.1 \times 10^{-4}\text{ s}^{-1}$ in the presence of PEG 1500. Similarly, the increase in the amount of CTABr coated Fe_3O_4 nanoparticles decreased the rate constant values from $4.0 \times 10^{-4}\text{ s}^{-1}$ to $1.02 \times 10^{-4}\text{ s}^{-1}$ in the presence of PEG 1500. The binding constant and rate constant were found to be lower in SDS coated nanoparticles than the CTABr coated particles. The observed results for k_{ψ} - [surfactant] in the presence of magnetic nanoparticles and surfactant coated nanoparticles were treated using the pseudophase kinetic model.

Introduction

Magnetic nanoparticles presents many interesting properties that can be used in a wide variety of applications including catalysis, magnetic seals and inks, magnetic recording media, ferrofluids, targeted drug delivery, contrast agents for magnetic resonance imaging and therapeutic agents for cancer treatment and in biomedicine etc. [1-3]. These applications require the properties like specific sizes, shapes, surface characteristics and magnetic properties of the nanomaterials [4]. Magnetite nanoparticles has considerable role in the targeted drug delivery also [5-8]. These nanocatalysts have the ability to catalyze the organic reactions involving oxidations, carbon-carbon coupling reactions, hydro-formylation reactions, epoxidation reactions, etc. [9-10]. The surface of the magnetic nanoparticles are often modified by coating with polymers, surfactants, starch, polyelectrolytes, etc. to enable them more suitable for cell separation, protein purification, environment and food analysis, organic and biochemical synthesis, industrial waste water treatment and in bio sciences, etc. [11-14]. The iron oxide nanoparticles are among the materials having more stability, more selective and efficient nanoparticles. It can be easily separated and recovered from the reaction medium by an external magnetic field.

Tetracaine is an ester containing drug which hydrolysed to form the para-aminobenzoic acid and dimethyl aminoethanol as primary metabolites. Tetracaine

(amethocaine) is used to numb different parts of the body such as eyes, nose, throat, skin, etc. by blocking nerve signals and thus reduces the sensation of pain [15-17]. It is also used as popular spinal anesthesia. Its topical analgesic properties make it useful ophthalmic anaesthesia. Delivery of the anaesthetic drugs to the target has always been a challenging issue. Drug delivery through the nanoparticles to the target has been the subject of studies by large number of workers in the recent years [18-21]. Drug formulations containing nanoparticles require an extensive kinetics studies to explore the stabilities under the varying sets of conditions. Informations pertaining to the stability of drug with nanoparticles, degree of association, degradation products formed and the mechanism of the reaction can be investigated through the kinetics studies.

The present studies were undertaken with the aim to get an insight into the chemical stability, dispensability, and binding ability of tetracaine with iron oxide nanoparticles. Tetracaine degradation rates in the presence of Fe_3O_4 and Fe_3O_4 coated with surfactants (with cetyltrimethyl ammonium bromide; CTABr@ Fe_3O_4 and sodium dodecyl sulphate; SDS@ Fe_3O_4) under the different reaction conditions will provide further informations regarding the mechanism of the degradation of tetracaine and the nature of products formed. The partitioning of tetracaine in the different pseudophases can be obtained with the help of the analysis of the variation in the reaction rates in the presence of surfactants through the applications of pseudophase and pseudophase ions exchange models. Thus, the present

investigations may be useful to develop the technique to deliver the drug with the help of nanoparticles to the target.

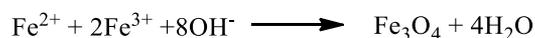
Experimental

Materials

Ferrous chloride dehydrate (99%; CDH, New Delhi), Ferric chloride (97.0%; CDH, New Delhi, India), liquor ammonia 25% (Thermo Fisher Scientific, Mumbai, India), Sodium hydroxide pellets (97%, Merck, Mumbai, India), CTABr (99%, CDH, New Delhi, India), Tetracaine (98%, TCI, Tokyo, Japan) and SDS (99%; CDH, New Delhi, India) were taken as supplied. All the other chemicals were used as such for the experimental work without further purification. Doubly distilled water was used for the preparation of various solutions of NaOH, SDS, CTABr, and ammonia. The stock solution of sodium hydroxide (1.0 mol dm^{-3}) was prepared in distilled water. The stock solutions of CTABr ($1.0 \times 10^{-2} \text{ mol dm}^{-3}$) and SDS ($1.0 \times 10^{-2} \text{ mol dm}^{-3}$) were prepared in doubly distilled water. Stock solution of tetracaine ($1.0 \times 10^{-3} \text{ mol dm}^{-3}$) was prepared in 99.9% ethanol.

Synthesis of Fe_3O_4 magnetic nanoparticles by co-precipitation method

Magnetic nanoparticles have been synthesized by using co-precipitation method [22-24]. 20.0 g of FeCl_3 (0.4M) and 10.0 g of $\text{FeCl}_2 \cdot 2\text{H}_2\text{O}$ (0.2M) were taken into a 1000 mL conical flask containing 300 mL doubly distilled water. The mixture was purged with N_2 gas to remove dissolved oxygen from the solution. The mixture was stirred for 60 minutes in order to mix Fe^{3+} and Fe^{2+} ions properly. Then, added 200 mL of 25% ammonium hydroxide solution drop wise into the conical vessel. To keep the environment inert, the N_2 gas was passed into the mixture and over the surface. 2M of NaOH solution was then added to the mixture to raise the pH further high (~14). The temperature of the conical flask was raised to 70°C by heating on water bath and N_2 gas was purged through the mixture. The precipitate appeared in the conical flask. It was filtered and washed with acetone and double distilled water. After filtration, the precipitate was left in a hot air oven at 70°C for ~5 hours. The synthesized nanoparticles were black in appearance. The formation of nanoparticles can be represented by the following reaction:



The synthesized nanoparticles were characterized to ensure the required material formation. In this precipitation method, the presence of traces of dissolved oxygen should be avoided through purging nitrogen gas otherwise the required product cannot be obtained.

Synthesis of CTABr-modified and SDS-modified magnetic nanoparticles

0.40 M $\text{FeCl}_3 \cdot 6\text{H}_2\text{O}$ (20 g), 0.20 M $\text{FeCl}_2 \cdot 4\text{H}_2\text{O}$ (10 g) and 0.10 M CTABr (10.92 g) were taken into conical flask of 1.0 L capacity containing 300 mL doubly distilled water.

The overhead stirrer was used to mix these materials properly. The solution was stirred vigorously for 45 minutes under the atmosphere of nitrogen gas. Then 200 mL of 25% ammonium hydroxide solution was added drop wise into the above solution until the pH of the resulting solution reached 9-11. The pH of the reaction medium was further raised to 14 by adding 2.0 M NaOH solution drop wise. This mixture was then stirred vigorously under purging nitrogen gas for five hours. The black precipitate formed was filtered and washed with distilled water several times. To prepare SDS-modified Fe_3O_4 MNPs, the same procedure was adopted by using aqueous solutions of 0.10 M (8.64 g) SDS instead of CTABr solution in the above experiment.

Equipments used for the characterizations of the synthesized CTABr-modified Fe_3O_4 and SDS-modified MNPs

The X-ray Diffraction (XRD) studies on the synthesized Fe_3O_4 MNPs were carried out by using X-ray Diffractometer, MiniFlex II, Rigaku, Japan, equipped with a Cu K_α radiation source ($\lambda = 1.5406 \text{ nm}$). The FT-IR spectra of the nanoparticles were recorded by Nicolet iS50 FT-IR Spectrometer (Thermo Fisher Scientific, Madison, USA). Field Emission Scanning Electron Microscope (FESEM, JSM-7800F, JEOL, Japan) and Transmission Electron Microscope (HRTEM, Techno, FEI) were used for the characterization of nanoparticles, Vibrating Sample magnetometer (VSM LakeShore-7404) was used to measure the magnetic behaviour of MNPs.

Kinetic experiments

Genesis 10S UV/Visible spectrophotometer (Thermo Fisher Scientific, Madison, USA) having multiple cell holders were used to perform all the kinetic experiments. The absorbance of the samples were measured using a quartz cuvette of volume 3.0 mL and path length of 10 mm. Thermo stated water-bath was used to equilibrate all the kinetics runs at constant temperature. The repetitive scans were recorded (Fig. 1) for the tetracaine hydrolysis in alkaline medium at the regular gap of 5 minutes for the mixture containing the solutions of tetracaine ($= 4.0 \times 10^{-5} \text{ mol dm}^{-3}$) and NaOH ($= 5.0 \times 10^{-2} \text{ mol dm}^{-3}$) at fixed temperature of 37°C . The requisite amounts of the reaction mixtures (tetracaine, surfactant and nanoparticles) were taken in a three necked round bottom flask with a capacity of 100 mL. The conical flasks containing tetracaine, surfactant, polyethylene glycol, NaOH were placed on the water-bath for 15 minutes to equilibrate the temperature before mixing them in a round bottom flask. The monitoring time of the reaction was started when 50 % of the total of requisite quantity of the NaOH was mixed with the other reactants. Pseudo-first-order conditions with $[\text{OH}^-] \gg [\text{tetracaine}]$ were maintained throughout the experiment. The decrease in absorbance at 315 nm was used as a parameter to trace the progression of the reaction. $\ln(\text{absorbance})$ versus time were plotted and its slope was used to calculate the pseudo-first-order rate

constants. Triplicate run of each kinetic experiment were performed with the reproducible values of rate constant having error limits of approximately 5%.

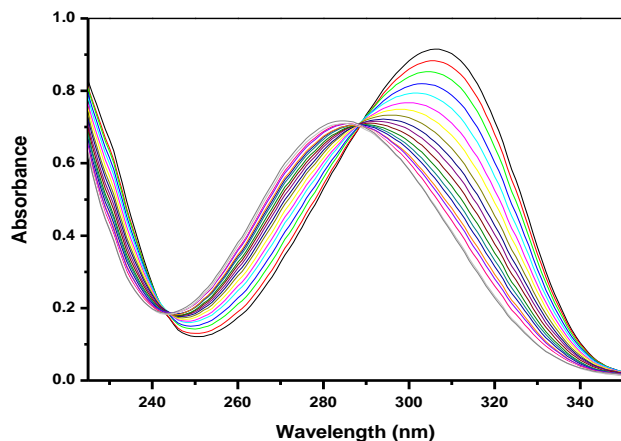


Fig. 1. The repetitive scans of the solution of tetracaine and NaOH at the interval of 5 minutes. Reaction conditions: [Tetracaine] = 4.0×10^{-5} mol dm^{-3} , [NaOH] = 5.0×10^{-2} mol dm^{-3} , Temperature = 37 °C.

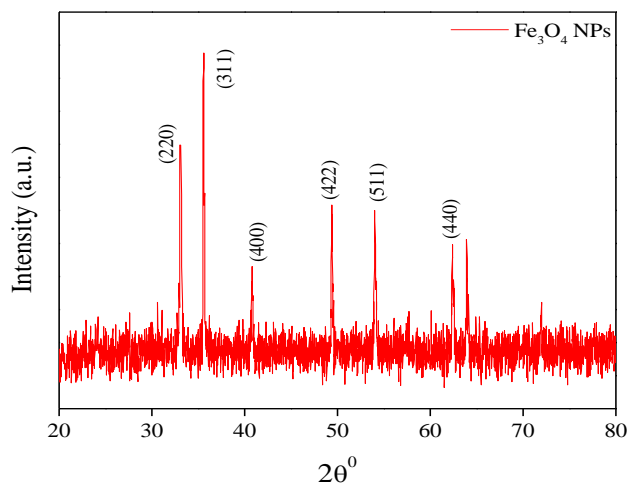


Fig. 2. The X-rays diffraction patterns obtained for Fe₃O₄.

Results and discussion

Characterizations

X-ray Diffraction (XRD)

The XRD patterns obtained for Fe₃O₄ are presented in Fig. 2, confirm the crystalline structure and phase purity of Fe₃O₄ nanoparticles. The diffraction peaks for 2θ values appeared at 30.26°, 35.5°, 43.12°, 53.74°, 57.10° and 62.92° which correspond to planes (220), (311), (400), (422), (511) and (440), respectively. The size of the particles was calculated by using the Scherrer Formula [25].

$$D = \frac{K\lambda}{\beta \cos\theta} \quad (1)$$

Here, in this equation, λ is the wavelength of X-rays (λ = 1.5406 nm), β is the full width at half maximum (FWHM) value, K is Scherrer constant (0.89), θ is the angle of diffraction and D is the particle diameter size. The average particle size of Fe₃O₄ determined by using equation (1) was found to be 14.82 nm.

Fourier Transform Infrared Spectroscopy (FTIR)

The FT-IR spectra of Fe₃O₄, CTABr modified Fe₃O₄ (CTABr@Fe₃O₄) and SDS modified Fe₃O₄ (SDS@Fe₃O₄) are shown in Fig. 3. The presence of two strong absorption bands at 635 cm⁻¹ and 585 cm⁻¹ correspond to the Fe-O bond vibration in Fe₃O₄ [26]. The appearance of absorption peak at 3424 cm⁻¹ is due to the O-H stretching vibration of hydroxyl group of water molecules associated with Fe₃O₄ [27]. The H-O-H bending of adsorbed water is visible by the appearance of peak at 1631 cm⁻¹ in the Fe₃O₄ nanoparticles [28]. The CTABr@Fe₃O₄ nanoparticles display a peak at 582 cm⁻¹ which corresponds to Fe-O. The presence of alkyl chains of CTABr appears at symmetric band at 1395 cm⁻¹. The two peaks at 2845 cm⁻¹ and 2922 cm⁻¹ are attributed to two different band vibration of CTABr [29]. Antisymmetric vibrations of N(CH₃)⁺, C-N, and CH₃⁺ stretching are found at 3015 cm⁻¹, 960 cm⁻¹ and 1465 cm⁻¹ [30]. The FTIR spectrum of SDS@Fe₃O₄ nanoparticles displays a new absorption peak at 1252 cm⁻¹ due to the stretching vibration of S=O groups of SDS and the presence of peaks at 2929 cm⁻¹ and 2842 cm⁻¹ are assigned to the stretching mode for aliphatic C-H groups of SDS [31]. The presence of peak at 529 cm⁻¹ is attributed to Fe-O of Fe₃O₄ [32]. The FTIR studies confirm the successful synthesis of Fe₃O₄ and their surface modifications through the adsorption of surfactants SDS and CTABr.

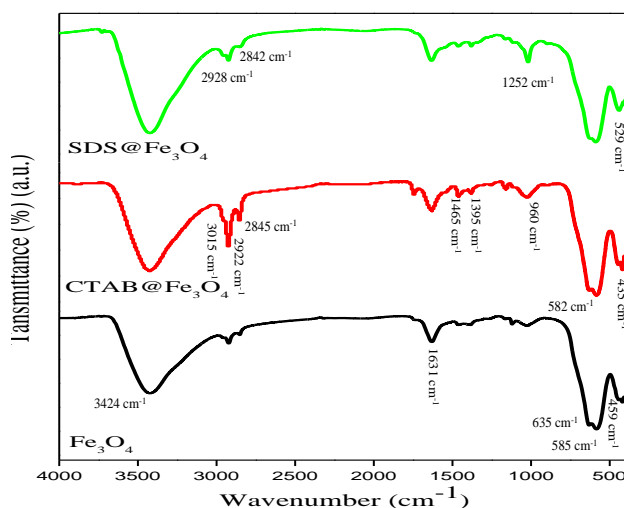


Fig. 3. The FT-IR spectra of Fe₃O₄, CTABr@Fe₃O₄ and SDS@Fe₃O₄

Scanning Electron Microscopy (SEM)

The SEM studies performed for the Fe₃O₄ nanoparticles, CTABr@Fe₃O₄ and SDS@Fe₃O₄ show that these nanoparticles have spherical irregular shape (Fig. 4). The CTABr@Fe₃O₄ and SDS@Fe₃O₄ nanoparticles are smaller in size as compared to that of Fe₃O₄ particles, due to the agglomeration of many ultrafine particles. It can be observed that nanoparticles have the spherical morphology with low polydispersity and particle size lower than 100 nm as shown in Figs. 4(a-c).

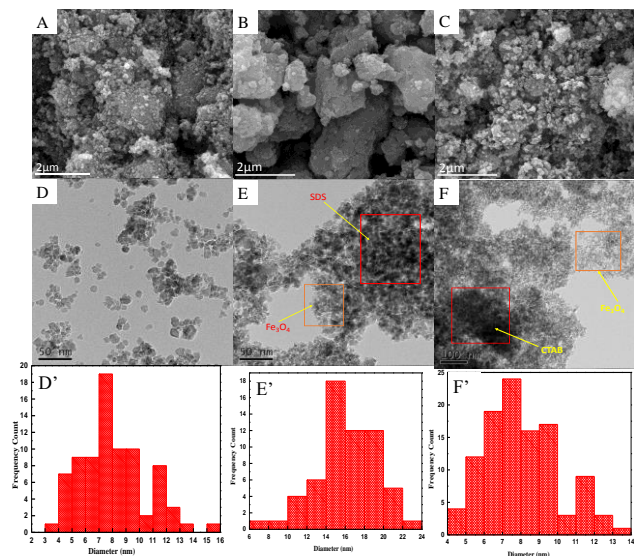


Fig. 4. SEM images of Fe_3O_4 (A); SDS@ Fe_3O_4 (B) and CTABr@ Fe_3O_4 (C); TEM images Fe_3O_4 (D); SDS@ Fe_3O_4 (E); CTABr@ Fe_3O_4 (F); Histogram images showing the size Fe_3O_4 (D);SDS@ Fe_3O_4 (E), CTABr@ Fe_3O_4 (F).

Transmission Electron Microscopy (TEM)

The TEM images of Fe_3O_4 are shown in **Fig. 4(d)**. The particles are spherical in shapes and the sizes vary in the range 10-20 nm. Thus, a good agreement is observed in the shape and particle size for Fe_3O_4 by TEM and XRD spectrum calculated by using Scherrer Formula. The TEM images of CTABr@ Fe_3O_4 and SDS@ Fe_3O_4 are shown in Figs. 4 (E-F). These images show a significant difference between the bare and modified nanoparticles. The coatings of Fe_3O_4 by CTABr and SDS reduce the particle size (CTABr@ $\text{Fe}_3\text{O}_4 \sim 8$ nm; SDS@ $\text{Fe}_3\text{O}_4 \sim 14$ nm).

Vibrating Sample Magnetometer (VSM)

The magnetic behavior of the Fe_3O_4 shows the saturation magnetization of nanoparticles at 40.00 emu/g (**Fig. 5**). This study indicates a very high saturation magnetization and super paramagnetic behavior of the nanoparticles [33].

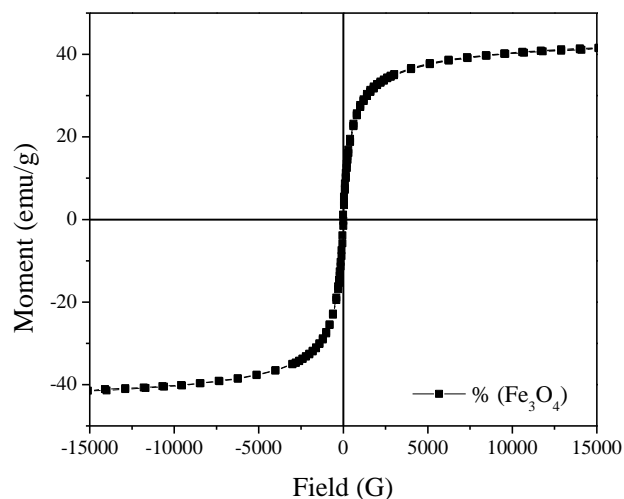


Fig. 5. Hysteresis curve for Fe_3O_4 at room temperature.

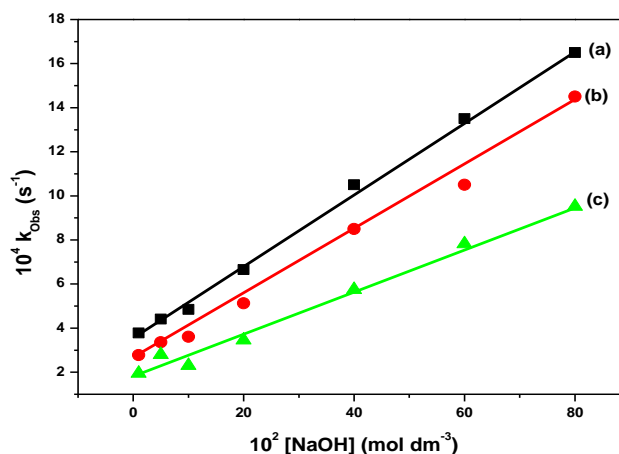
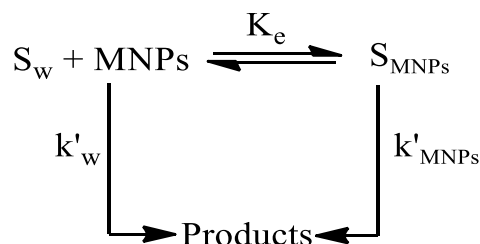


Fig. 6. Plots of k_{obs} versus $[\text{NaOH}]$ in the absence of Fe_3O_4 (a); in the presence of 0.2% (w/v) Fe_3O_4 (b) and 0.4% (w/v) Fe_3O_4 (c). Reaction conditions: $[\text{Tetracaine}] = 4.0 \times 10^{-5} \text{ mol dm}^{-3}$ and Temperature = 37°C .

Influence of Fe_3O_4 nanoparticles and Surfactants on the Alkaline Hydrolysis of Tetracaine

The added iron nanoparticles into the solution containing NaOH and tetracaine decreased the rate constant values. The kinetics studies were performed using 0.2 % and 0.4 % (w/v) Fe_3O_4 at varying concentration of sodium hydroxide in the range from $1.0 \times 10^{-2} \text{ mol dm}^{-3}$ to $8.0 \times 10^{-1} \text{ mol dm}^{-3}$. **Fig. 6** shows that the values of rate constant increased with increase in the concentration of sodium hydroxide. The values of rate constant in the presence of Fe_3O_4 were found to be lower than the corresponding values obtained in the absence of Fe_3O_4 . The amount of Fe_3O_4 was changed from 0.02 % to 0.40 % (w/v) keeping tetracaine and sodium hydroxide fixed at $4.0 \times 10^{-5} \text{ mol dm}^{-3}$ and 5.0×10^{-2} accordingly. It has been observed that the increase in amount of Fe_3O_4 particles decreased rate constant values. The decrease in the rate constant values for the alkaline hydrolysis of tetracaine in the presence of Fe_3O_4 may be attributed to the inhibitive effect of Fe_3O_4 surfaces. The Fe_3O_4 may able to adsorb OH^- ions and or tetracaine or both. The tetracaine molecules may get adsorbed to Fe_3O_4 and become less active for hydrolysis and so the reaction rate for the hydrolysis of tetracaine decreases. The tetracaine molecules in the presence of Fe_3O_4 are distributed into the aqueous medium and some of the molecules are adsorbed with Fe_3O_4 surface. The adsorption of tetracaine on Fe_3O_4 surface makes it unavailable for the OH^- ions attack and therefore the rate of reaction for the hydrolysis of tetracaine decreases. The following mechanism is proposed (**Scheme 1**).



Scheme 1

Where, S_w denotes free tetracaine present in the aqueous medium and S_{MNP_s} is the Fe_3O_4 bound tetracaine. K_e is the equilibrium constant for the distribution of tetracaine occurring in the aqueous and adsorbed phase. The mechanism of the reaction is shown in Scheme 1, the overall reaction rate of given by:

$$\text{Rate} = k'_w S_w + k'_{MNP_s} S_{MNP_s} \quad (2)$$

where, k'_w and k'_{MNP_s} are the first order reaction rate constant for the hydrolysis of tetracaine. The equilibrium distribution of tetracaine in aqueous medium and Fe_3O_4 bound can be given by equation (3)

$$K_e = \frac{[S_{MNP_s}]}{[S_w][MNP_s]} \quad (3)$$

Equation (1) can be rewritten as

$$\text{Rate} = k'_w S_w + k'_{MNP_s} K_e S_w [MNP_s] \quad (4)$$

The total concentration of tetracaine is

$$[S_w]_T = [S_w] + [S_{MNP_s}] \quad (5)$$

Or,

$$[S_w]_T = [S_w] + K_e [S_w][MNP_s] \quad (6)$$

Also, the rate of reaction for the alkaline hydrolysis in terms of primary tetracaine concentration, $[S_w]_T$ is given by

$$\text{Rate} = k_\psi [S_w]_T \quad (7)$$

Where, k_ψ is the first order reaction rate constant and its values in terms of k'_w and k'_{spion} can be deduced by using equations (4) and (6).

Or,

$$k_\psi = \frac{k'_w + k'_{MNP_s} K_e [MNP_s]}{1 + K_e [MNP_s]} \quad (8)$$

On rearrangement of equation (7), we get:

$$\frac{1}{k'_w - k_\psi} = \frac{1}{k'_w - k'_{MNP_s}} + \frac{1}{(k'_w - k'_{MNP_s}) K_e [MNP_s]} \quad (9)$$

The plot of $\frac{1}{k'_w - k_\psi}$ versus $\frac{1}{[MNP_s]}$ of equation (9) was used to determine the equilibrium constant (K_e) for the binding of tetracaine with Fe_3O_4 from the slope of the plot. The values of k'_{MNP_s} were calculated from the intercept and are given in **Table 1**.

Table 1. Values of K_e obtained from the plots of $\frac{1}{k'_w - k_\psi}$ versus $\frac{1}{[MNP_s]}$

Magnetic Nanoparticles	K_e	$10^5 k'_{MNP_s} (s^{-1})$
Fe_3O_4	7.44	12.3
CTABr@ Fe_3O_4	38.7	9.8
SDS@ Fe_3O_4	42.4	2.5

Reaction conditions: $[Tetracaine] = 4.0 \times 10^{-5} \text{ mol dm}^{-3}$ $[NaOH] = 5.0 \times 10^{-2} \text{ mol dm}^{-3}$ and Temperature = 37 °C.

The influence of surfactants on the values of rate constants was also studied. The increase in surfactant concentration (CTABr and SDS) into the solution containing, tetracaine, NaOH and Fe_3O_4 decreased rate of reaction for the hydrolysis of tetracaine. The [surfactant] was increased from $1.0 \times 10^{-2} \text{ mol dm}^{-3}$ to $5.0 \times 10^{-2} \text{ mol dm}^{-3}$

in the presence of 0.2 % and 0.4 % (w/v) Fe_3O_4 . Under the set of reaction condition, besides Fe_3O_4 , the other micro-heterogeneous phases are micellar pseudophase and aqueous pseudophase. Tetracaine molecules are either solubilized into aqueous and micellar phases or adsorbed to the Fe_3O_4 surfaces. Similarly, some of the surfactant molecules are also adsorbed to the Fe_3O_4 surfaces and help to adsorb the tetracaine molecules more towards the Fe_3O_4 surfaces. Therefore, more inhibitive effect is found on the reaction rates for the alkaline hydrolysis of tetracaine in the presence of CTABr (**Fig. 7**). The reaction rate for the alkaline hydrolysis of tetracaine increases with increment in the concentration of SDS at constant $[NaOH]$ in the presence of 0.2 % and 0.4 % (w/v) Fe_3O_4 (**Fig. 8**). The increase in the rate of hydrolysis may be due to the poor binding of tetracaine with SDS and Fe_3O_4 surfaces and also due to the more competitive binding of hydroxide ions with the anionic SDS micelles and Fe_3O_4 nanoparticles and thus tetracaine remains mostly in the aqueous phase.

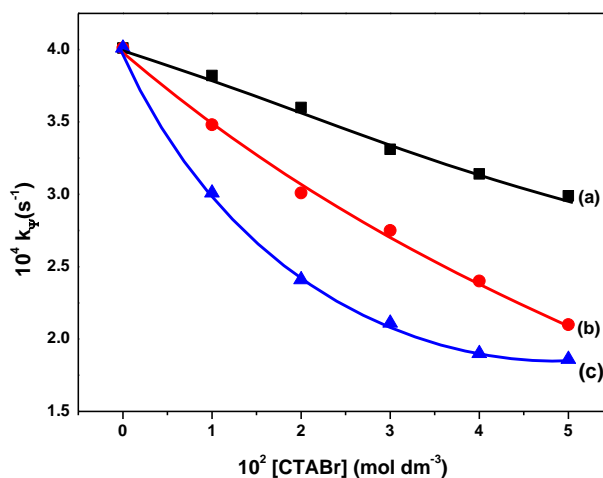


Fig. 7. Plots of k_ψ versus $[CTABr]$ in the absence of Fe_3O_4 (a); in the presence of Fe_3O_4 0.2% (w/v)(b) and (0.4% w/v) (c) Fe_3O_4 . Reaction conditions: $[Tetracaine] = 4.0 \times 10^{-5} \text{ mol dm}^{-3}$, $[NaOH] = 5.0 \times 10^{-2} \text{ mol dm}^{-3}$ and Temperature = 37 °C.

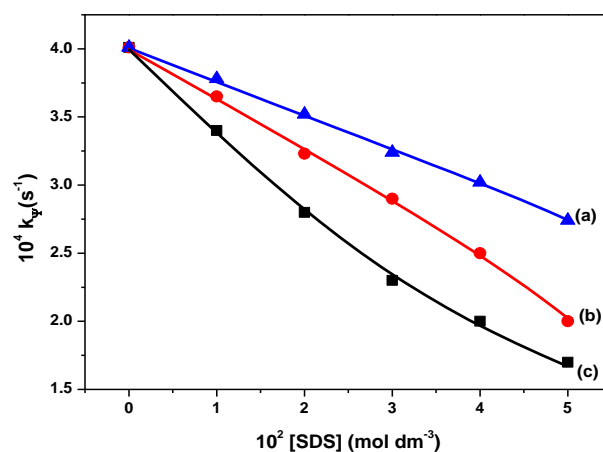


Fig. 8. Plots of k_ψ versus $[SDS]$ in the absence of Fe_3O_4 (c); in the presence of Fe_3O_4 0.2% (w/v)(b) and (0.4% w/v) (a) Fe_3O_4 . Reaction conditions: $[Tetracaine] = 4.0 \times 10^{-5} \text{ mol dm}^{-3}$, $[NaOH] = 5.0 \times 10^{-2} \text{ mol dm}^{-3}$ and Temperature = 37 °C.

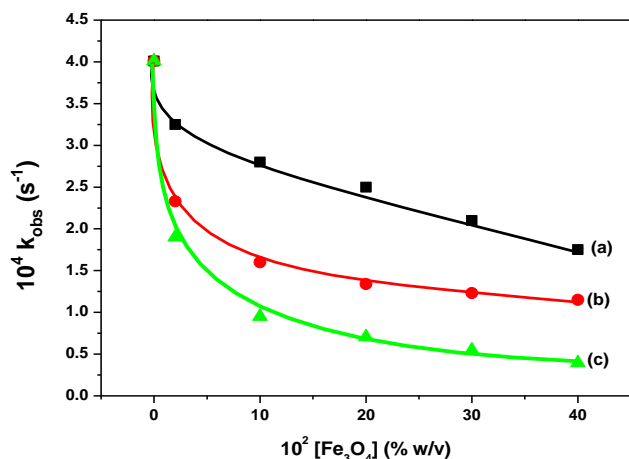


Fig. 9. Plots of k_{obs} versus $[Fe_3O_4]/[surfactant\ coated\ Fe_3O_4]$. (a) = $[Fe_3O_4]$, (b) = $[CTABr@Fe_3O_4]$, and (c) = $[SDS@Fe_3O_4]$. Reaction conditions: $[Tetracaine] = 4.0 \times 10^{-5} mol\ dm^{-3}$, $[NaOH] = 5.0 \times 10^{-2} mol\ dm^{-3}$ and Temperature = $37\ ^\circ C$.

Effect of Surfactant-Modified Iron Nanoparticles and Polyethylene glycol mixture on the Alkaline Hydrolysis of Tetracaine

Fig. 9 shows the trend in deviation for the reaction rate constant values with increment in the amount of the surfactant coated Fe_3O_4 . Therefore, the reaction rate constant values show a greater inhibitive effect for $SDS@Fe_3O_4$ as compared to $CTABr@Fe_3O_4$. The mechanism of the reaction is assumed to be the same as proposed in Scheme 1 and the observed results were treated using the relationship given in equation (9). The values of rate constant and equilibrium constant for surfactant coated Fe_3O_4 are given in Table 1. The higher values of equilibrium constant for the binding of tetracaine with SDS than CTABr suggest that more tetracaine molecules are adsorbed with SDS coated Fe_3O_4 . The reaction rate constant values decreased with increase in the amount of polyethylene glycols (PEG) of molecular weights of 1500, 4000, 6000 and 8000 in the presence $CTABr@Fe_3O_4$ and $SDS@Fe_3O_4$ nanoparticles. The amount of $SDS@Fe_3O_4$ and $CTABr@Fe_3O_4$ was increased from 0.02 to 0.4% (w/v) at a constant polyethylene glycol concentration that is 1% (w/v). The concentrations of tetracaine ($4.0 \times 10^{-5} mol\ dm^{-3}$) and sodium hydroxide ($5.0 \times 10^{-2} mol\ dm^{-3}$) were kept constant at $37\ ^\circ C$ respectively. The change in rate constant values against the varying amount of $SDS@Fe_3O_4$ and $CTABr@Fe_3O_4$, are given in **Table 2** and **Table 3** respectively. The values of equilibrium constant and reaction rate constant obtained at varying concentration of $SDS@Fe_3O_4$ and $CTABr@Fe_3O_4$ at a fixed PEG concentration of different molecular weights are given in **Table 4**. The increase in the concentration of PEG at fixed $CTABr@Fe_3O_4$ and $SDS@Fe_3O_4$ also decreased reaction rate for the hydrolysis of tetracaine. The values of equilibrium constant and rate constant obtained at these PEG concentrations and at fixed amount of surfactant coated iron nanoparticles ($SDS@Fe_3O_4$ and $CTABr@Fe_3O_4$) are given in **Tables 5-6**.

Table 2. Variation in the values of rate constant (k_{obs}) as a function of amount of $SDS@Fe_3O_4$ in the presence of 1.0% (w/v) PEGs of different molecular weights.

$10^2 [SDS@Fe_3O_4]$ (% w/v)	$10^4 k_{obs} (s^{-1})$			
	PEG 1500	PEG 4000	PEG 6000	PEG 8000
0	4.01	4.01	4.01	4.01
2	3.01	2.3	1.7	1.2
10	1.9	1.52	0.925	0.52
20	1.37	1.1	0.75	0.39
30	1.21	0.955	0.622	0.33
40	1.1	0.878	0.455	0.233

Reaction conditions: $[Tetracaine] = 4.0 \times 10^{-5} mol\ dm^{-3}$, $[NaOH] = 5.0 \times 10^{-2} mol\ dm^{-3}$ and Temperature = $37\ ^\circ C$.

Table 3. Variation in the values of rate constant (k_{obs}) as a function of amount of $CTABr@Fe_3O_4$ in the presence of 1.0% (w/v) PEGs of different molecular weights.

$10^2 [CTABr@Fe_3O_4]$ (% w/v)	$10^4 k_{obs} (s^{-1})$			
	PEG 1500	PEG 4000	PEG 6000	PEG 8000
0	4.01	4.01	4.01	4.01
2	2.5	2.1	1.35	1.2
10	1.52	0.976	0.756	0.49
20	1.27	0.726	0.426	0.309
30	1.12	0.615	0.342	0.214
40	1.02	0.515	0.233	0.101

Reaction conditions: $[Tetracaine] = 4.0 \times 10^{-5} mol\ dm^{-3}$, $[NaOH] = 5.0 \times 10^{-2} mol\ dm^{-3}$ and Temperature = $37\ ^\circ C$.

Table 4. Variation in the values of rate constant (k_{obs}) with the increase in [PEGs] of different molecular weights in the presence of $SDS@Fe_3O_4$ (0.1% w/v) and $CTABr@Fe_3O_4$ (0.1% w/v).

[PEG] (w/v)	$10^4 k_{obs} (s^{-1})$							
	PEG 1500		PEG 4000		PEG 6000		PEG 8000	
	SDS@ Fe_3O_4	CTABr @ Fe_3O_4	SDS @ Fe_3O_4	CTA Br@ Fe_3O_4	SDS@ Fe_3O_4	CTA Br@ Fe_3O_4	SDS@ Fe_3O_4	CTABr @ Fe_3O_4
0	4.01	4.01	4.01	4.01	4.01	4.01	4.01	4.01
0.5	2.5	2.25	2.3	1.8	2.1	1.5	1.8	1.3
1	1.85	1.52	1.61	1.1	1.41	0.756	1.2	0.49
1.5	1.63	1.3	1.25	0.825	1.1	0.645	0.75	0.35
2	1.52	1.2	1.13	0.777	0.825	0.522	0.52	0.28
2.5	1.41	1.1	1.07	0.678	0.666	0.42	0.23	0.22

Reaction conditions: $[Tetracaine] = 4.0 \times 10^{-5} mol\ dm^{-3}$, $[NaOH] = 5.0 \times 10^{-2} mol\ dm^{-3}$ and Temperature = $37\ ^\circ C$.

Table 5. Variation in the values of K_e and k_{MNP} s with the change in the amount of $CTABr@Fe_3O_4$ and $SDS@Fe_3O_4$ in the presence of fixed [PEGs].

Kinetic Parameter	PEG1500		PEG4000		PEG6000		PEG8000	
	CTABr @ Fe_3O_4	SDS @ Fe_3O_4	CTABr @ Fe_3O_4	SDS @ Fe_3O_4	CTABr @ Fe_3O_4	SDS @ Fe_3O_4	CTABr @ Fe_3O_4	SDS @ Fe_3O_4
K_s	51.4	23	49.3	26.6	45.9	96.2	130	145
$10^3 k_m (s^{-1})$	9.45	8.47	3.69	5.66	4.63	5.13	1.30	2.39
R^2	0.998	0.998	0.988	0.999	0.994	0.983	0.985	0.993

Reaction conditions: $[Tetracaine] = 4.0 \times 10^{-5} mol\ dm^{-3}$, $[NaOH] = 5.0 \times 10^{-2} mol\ dm^{-3}$ [PEG] = 1% w/v and Temperature = $37\ ^\circ C$.

Table 6. Variation in the values of K_e and k_{MNP} s with the change in [PEGs] in the presence of fixed amount of $CTABr@Fe_3O_4$ and $SDS@Fe_3O_4$.

Kinetic Parameter	PEG1500		PEG4000		PEG6000		PEG8000	
	CTABr @ Fe_3O_4	SDS @ Fe_3O_4	CTABr @ Fe_3O_4	SDS @ Fe_3O_4	CTABr @ Fe_3O_4	SDS @ Fe_3O_4	CTABr @ Fe_3O_4	SDS@ Fe_3O_4
K_s	197	177	385	218	567	170	756	141
$10^3 k_m (s^{-1})$	4.22	7.58	3.27	4.79	2.03	0.969	0.263	0.784
R^2	0.985	0.990	0.972	0.974	0.949	0.993	0.998	0.994

Reaction conditions: $[Tetracaine] = 4.0 \times 10^{-5} mol\ dm^{-3}$, $[NaOH] = 5.0 \times 10^{-2} mol\ dm^{-3}$, $CTABr@Fe_3O_4$ and $SDS@Fe_3O_4$ at (0.1% w/v) and Temperature = $37\ ^\circ C$.

Conclusion

The iron oxide nanoparticles were synthesized by coprecipitation method and the synthesized material was characterized by different physical techniques. The XRD patterns showed the crystalline nature of the material. The appearance of additional band at 1252 cm^{-1} ensured the coatings of iron nanoparticles with SDS. Similarly, the band at 960 cm^{-1} , 1395 cm^{-1} , and 1465 cm^{-1} confirmed the coating of materials by CTABr. The rates of reaction for the alkaline hydrolysis of tetracaine was found to be independent on [tetracaine] but increased linearly with the increment in the [NaOH]. The increase in the amount of Fe_3O_4 decreased the rate of reaction. The decreasing effect on the rate of reaction for the hydrolysis of tetracaine was observed on increasing the concentration of CTABr and SDS in the presence of Fe_3O_4 . The same trend of decrease in the rate of reaction was followed on increasing the amount of surfactant coated Fe_3O_4 nanoparticles. The added PEGs solution in the presence of Fe_3O_4 and surfactant coated Fe_3O_4 displayed inhibitive effect on the reaction rate. The analysis of the kinetic results showed the higher binding ability of tetracaine with Fe_3O_4 nanoparticles and with surfactant coated Fe_3O_4 nanoparticles. These findings can be further explored to use Fe_3O_4 nanoparticles and surfactant coated Fe_3O_4 nanoparticles as drug carrier. Further, the study establishes that the drug is more stable in the presence of these nanoparticles.

Acknowledgments

The authors are thankful to UGC, New Delhi for providing scholarship and contingency for the progress of the research work.

Keywords

Base catalysed hydrolysis of tetracaine, Fe_3O_4 magnetic nanoparticles, SDS@ Fe_3O_4 , CTABr@ Fe_3O_4

Received: 6 July 2020

Revised: 18 July 2020

Accepted: 21 July 2020

References

- Godoi, M.; Liz, D. G.; Ricardo, E. W.; Rocha, M. S. T.; Azeredo, J. B.; Braga, A. L.; *Tetrahedron*, **2014**, *70*, 3349.
- Kumar, A.; Gupta, M.; *Biomaterials*, **2005**, *26*, 3995.
- Alishiri, T.; Oskooei, H. A.; Heravi, M. M.; *Synth. Commun.*, **2013**, *43*, 3357.
- Teja, A. S.; Koh, P. Y.; *Prog. Cryst. Growth Charact. Mater.*, **2009**, *55*, 22.
- Gonzales, M.; Krishnan, K. M.; *J. Magn. Magn. Mater.*, **2005**, *293*, 265.
- Ai, H.; Flask, C.; Weinberg, B.; Shuai, X. T.; Pagel, M. D.; Farrell, D.; Duerk, J.; Gao, J.; *Adv. Mater.*, **2005**, *17*, 1949.
- Jurgons, R.; Seliger, C.; Hilpert, A.; Trahms, L.; Odenbach, S.; Alexiou, C.; *J. Phys. Condens. Matter*, **2006**, *18*, S2893.
- Tartaj, P.; M. a del P. Morales; Veintemillas-Verdaguer, S.; Gonzalez-Carre o, T.; Serna, C. J.; *J. Phys. D. Appl. Phys.*, **2003**, *36*, R182.
- Mamani, J. B.; Gamarra, L. F.; de S. Brito, G. E.; *Mater. Res.*, **2014**, *17*, 542.
- Huang, J.; Wang, Y.; Hao, Z.; Peng, X.; *J. Saudi Chem. Soc.*, **2017**, *21*, 811.
- Kim, D. K.; Mikhaylova, M.; Wang, F. H.; Kehr, J.; Bjelke, B.; Zhang, Y.; Tsakalagos, T.; Muhammed, M.; *Chem. Mater.*, **2003**, *15*, 4343.
- Kohler, N.; Sun, C.; Wang, J.; Zhang, M.; *Langmuir*, **2005**, *21*, 8858.
- Zhang, J. L.; Srivastava, R. S.; Misra, R. D. K.; *Langmuir*, **2007**, *23*, 6342.
- Kievit, F. M.; Veiseh, O.; Bhattarai, N.; Fang, C.; Gunn, J. W.; Lee, D.; Ellenbogen, R. G.; Olson, J. M.; Zhang, M.; *Adv. Funct. Mater.*, **2009**, *19*, 2244.
- Brechner, V. L.; Cohen, D. D.; Pretsky, I.; *Ann. N. Y. Acad. Sci.*, **1967**, *141*, 524.
- Deupree, J.; *xPharm: The Comprehensive Pharmacology Reference*, Elsevier, **2007**, 1.
- Foldvari, M.; Gesztes, A.; Mezei, M.; Cardinal, L.; Kowalczyk, I.; Behl, M.; *Drug Dev. Ind. Pharm.*, **1993**, *19*, 2499.
- Rawat, M.; Singh, D.; Saraf, S.; *Biol. Pharm. Bull.*, **2006**, *29*, 1790.
- De Jong, W.H.; Borm, P.J.A.; *Int. J. Nanomedicine*, **2008**, *3*, 133.
- Ochekepe, N.A.; Olorunfemi, P.O.; Ngwuluka, N.; *Trop. J. Pharm. Res.*, **2009**, *8*, 265.
- Ochekepe, N.A.; Olorunfemi, P.O.; Ngwuluka, N.; *Trop. J. Pharm. Res.*, **2009**, *8*, 275.
- Márquez, F.; Herrera, G. M.; Campo, T.; Cotto, M.; Ducongé, J.; Sanz, J. M.; Elizalde, E.; Perales, O.; Morant, C.; *Nanoscale Res. Lett.*, **2012**, *7*, 210.
- Li, M. Y.; Sui, X. D.; *Key Eng. Mater.*, **2012**, *82*, 512.
- Azcona, P.; Zysler, R.; Lassalle, V.; *Colloids Surfaces A Physicochem. Eng. Asp.*, **2016**, *504*, 320.
- López, J.; González, F.; Bonilla, F.; Zambrano, G.; Gomez, M.; Synthesis and characterization of Fe_3O_4 magnetic nanofluid, **2010**, Vol. 30.
- Saranya, T.; Parasuraman, K.; Anbarasu, M.; Balamurugan, K.; *Nano Vis.*, **2015**, *5*, 149.
- Aliramaji, S.; Zamanian, A.; Sohrabijam, Z.; *Procedia Mater. Sci.*, **2015**, *11*, 265.
- Saif, B.; Wang, C.; Chuan, D.; Shuang, S.; *J. Biomater. Nanobiotechnol.*, **2015**, *6*, 267.
- Elfeky, S. A.; Ebrahim, S.; Fahmy, A.; *J. Adv. Res.*, **2017**, *8*, 435.
- Heidari A.; Noshin Mir.; Reza Nikkaran, Ali; *J. Nanostruct.*, **2016**, *6*, 199.
- Azari, Z.; Pourbasheer, E.; Beheshti, A.; *Spectrochim. Acta - Part A Mol. Biomol. Spectrosc.*, **2016**, *153*, 599.
- Bavili Tabrizi, A.; Dehghani Teymurloie, N.; *J. Mex. Chem. Soc.*, **2018**, *60*, 108.
- Mahmoudi, M.; Simchi, A.; Imani, M.; Ha, U. O.; *J. Phys. Chem. C*, **2009**, *113*, 8124.